

Large-scale metric objects filtering for binary classification with application to abnormal brain connectivity detection

Shuaida He¹, Jiaqi Li¹, and Xin Chen^{*1}

¹Department of Statistics and Data Science, Southern University of Science and Technology, Shenzhen, China

March 20, 2024

Abstract

The classification of random objects within metric spaces without a vector structure has attracted increasing attention. However, the complexity inherent in such non-Euclidean data often restricts existing models to handling only a limited number of features, leaving a gap in real-world applications. To address this, we propose a data-adaptive filtering procedure to identify informative features from a large-scale of random objects, leveraging a novel Kolmogorov–Smirnov-type statistic defined on the metric space. Our method, applicable to data in general metric spaces with binary labels, exhibits remarkable flexibility. It enjoys a model-free property, as its implementation does not rely on any specified classifier. Theoretically, it effectively controls the false discovery rate while guaranteeing the sure screening property. Empirically, equipped with a Wasserstein metric, it demonstrates superior sample performance compared to Euclidean competitors. When applied to analyze a dataset on autism, our method identifies significant brain regions associated with the condition. Moreover, it reveals distinct interaction patterns among these regions between individuals with and without autism, achieved by filtering hundreds of thousands of covariance matrices representing various brain connectivities.

1 Introduction

We consider metric binary classification, where features are represented as random objects in general metric spaces. Specifically, let $Y \in \{-1, 1\}$ be a class label and $X = (X_1, \dots, X_p)$ be an ordered p -tuple of features. Each X_j ($1 \leq j \leq p$) is assumed to be a random object from the metric space (\mathcal{M}_j, d_j) , where \mathcal{M}_j is a set, and d_j is the corresponding metric (or distance). When (\mathcal{M}_j, d_j) lacks an additional vector structure, it is often referred to as a non-Euclidean space. Typically examples include the space of symmetric positive definite (SPD) matrices (Lin, 2019), directional objects (Mardia et al., 2000), phylogenetic trees (Billera et al., 2001), subspaces like Grassmannians (Lim et al., 2021), and probability functions equipped with Wasserstein metric (Chen et al., 2023). Analyzing such non-Euclidean data poses inherent challenges due to the absence of extensive algebraic structures.

Binary classification, given a joint probability measure \mathbb{P} defined over $\mathcal{M} \times \{-1, +1\}$, seeks a function $h : \mathcal{M} \rightarrow \{-1, +1\}$ that minimizes the risk of $\mathbb{P}\{h(X) \neq Y\}$. Here, $\mathcal{M} = \prod_{j=1}^p \mathcal{M}_j$ denotes the Cartesian product space of \mathcal{M}_j , and the function h is usually constrained to a pre-specified class \mathcal{H} . Commonly employed classes \mathcal{H} include the Lipschitz large-margin classifiers (von Luxburg and Bousquet, 2004; Gottlieb et al., 2014), nearest neighbor classifiers (Cover and Hart, 1967; Chaudhuri and Dasgupta, 2014; Kontorovich et al., 2018), and metric logistic regression models (Lin and Lin, 2023), to name a few.

*Corresponding author: Xin Chen, chenx8@sustech.edu.cn

Despite their utility, these metric classifiers often suffer from limited computational efficiency, restricting their applicability to datasets with few features.

In many scenarios, a relatively small sample size n may coexist with a large or even huge value of p (e.g., $p = \exp\{O(n^\alpha)\}$ for some $\alpha > 0$), which is known as the curse of dimensionality in the Euclidean setting. Nonetheless, it is commonly believed that the underlying classification rule depends only on a few important features $\{X_j, j \in \mathcal{D}\}$, where \mathcal{D} represents a subset of $\{1, \dots, p\}$ with a cardinality d significantly smaller than n (e.g., $d = o(n)$), and is termed as the informative set. This assumption not only facilitates the effective handling of a large-scale of metric features but also provides a deeper understanding of the original classification problem. Our primary focus is on identifying such \mathcal{D} .

For Euclidean features, an effective solution involves leveraging the celebrated feature screening technique (Fan and Lv, 2008, 2018), extensively studied in the literature with diverse variants (Zhu et al., 2011; Mai and Zou, 2013; Cui et al., 2015). Essentially, feature screening aids in constructing a subset of features covering \mathcal{D} with high probability. A classic application is locating key genes contributing significantly to tumor classification using high-dimensional micro-array data. However, in scenarios where features are random objects in general metric spaces, the identification of \mathcal{D} becomes more challenging and remains relatively unexplored. To the best of our knowledge, the most promising approach so far is the ball correlation screening procedure (Pan et al., 2019), designed for objects in separable Banach spaces. Although it can be extended to metric spaces according to the Banach-Mazur theorem (Kleiber and Pervin, 1969), this extension is less straightforward and may lose some power in a binary classification setting.

In this paper, we estimate the informative set \mathcal{D} by developing an effective filtering procedure that operates on a large set of random objects in metric spaces with binary labels. This filtering procedure is designed to avoid relying on strong model assumptions, making it applicable to arbitrary classifier classes \mathcal{H} . Additionally, it exhibits flexibility to handle various metric spaces. To achieve this, we leverage a Kolmogorov–Smirnov-type statistic defined on the metric space. Our filtering procedure, based on this novel statistic, extends the approach proposed in Mai and Zou (2013) to the non-Euclidean setting. To balance classification performance and computational efficiency, the proposed method filters out as many irrelevant objects as possible while retaining informative features. We demonstrate this by showing that it enjoys the sure screening property while effectively controlling the false discovery rate, when combined with a data-adaptive threshold selection procedure.

As another contribution of this work, we apply the proposed method to detect abnormal functional connectivities in autism brains. We first construct a large pool of symmetric positive definite matrices as metric features to characterize various brain functional connectivities and then apply our filtering method. The identified informative features are highly interpretable, revealing significant differences in brain connectivity patterns between individuals with autism and controls. Some of these findings are less reported in existing autism studies and may warrant future investigation. Moreover, in the subsequent classification task, the classifier based on these informative features demonstrates significantly enhanced prediction performance under various criteria.

Besides binary classification, recent interest in non-Euclidean data analysis has also spurred the development of many other methods. These encompass Fréchet mean estimation in metric spaces (McCormack and Hoff, 2021), Fréchet linear regression (Petersen and Müller, 2019), Fréchet single index models (Bhattacharjee and Müller, 2023), sufficient dimension reduction for random objects (Ying and Yu, 2022; Zhang et al., 2023), functional models for time-varying random objects (Dubey and Müller, 2020), and more. Again, despite their wide range of applications, these methods are not specifically designed to handle a large-scale of non-Euclidean features.

2 Preliminaries

2.1 Examples of metric spaces

We briefly introduce some metric spaces that will be encountered later in the paper.

Example 1 (The Wasserstein space of univariate distributions). Let $(X, \mathcal{B}(X))$ be a measurable space, where X is either \mathbb{R} or a closed interval of \mathbb{R} , and $\mathcal{B}(X)$ is the associated Borel σ -field. The Wasserstein space $\mathcal{W}(X)$ is the set of probability distributions F on $(X, \mathcal{B}(X))$ such that $\int_X x^2 dF(x) < \infty$, equipped with quadratic Wasserstein distance $d_w(F_1, F_2) = (\int_0^1 [F_1^{-1}(s) - F_2^{-1}(s)]^2 ds)^{1/2}$, where $F_1, F_2 \in \mathcal{W}$ and F_1^{-1} and F_2^{-1} are the quantile functions corresponding to F_1 and F_2 , respectively. Then $(\mathcal{W}(X), d_w)$ is a metric space with a Riemannian structure (Chen et al., 2023).

Example 2 (The space of SPD matrices with a fixed dimension). Let \mathcal{S}_m^+ denote the set of $m \times m$ symmetric positive-definite (SPD) matrices. Generally, \mathcal{S}_m^+ forms a smooth submanifold embedded in $\mathbb{R}^{m(m+2)/2}$. When equipped with the inherited Euclidean metric, it becomes a Riemannian manifold. However, the determinant of Euclidean average of SPD matrices may larger than any of the original determinants, leading to the well-known phenomenon of swelling effect (Arsigny et al., 2007). This limitation, along with others, motivates the development of various alternative metrics for \mathcal{S}_m^+ , such as the Log-Euclidean metric, the Cholesky distance (Dryden et al., 2009), and the Log-Cholesky (Lin, 2019), among others. See illustrative examples in section 4.2.

2.2 Metric distribution function

Suppose X is a random object taking values in a general metric space (\mathcal{M}, d) and μ is the associated Borel probability measure. Throughout this article, we assume (\mathcal{M}, d) is a complete and separable (i.e., Polish) space without the linear structure. To perform nonparametric statistical inference on samples from this non-Euclidean space \mathcal{M} , Wang et al. (2023) introduced a fundamental tool termed metric distribution function (MDF). They proved that MDF, as a quasi-distribution function, uniquely determines μ when (\mathcal{M}, d) is a Polish space and d satisfies some mild conditions; see Theorem 1 in Wang et al. (2023) for details. This key result suggests that MDF can serve a role in metric space-based statistical inference akin to the distribution function in the Euclidean setting. We provide a brief review of MDF before moving on.

Roughly speaking, the metric distribution function is constructed upon all open balls in (\mathcal{M}, d) , which is a base of the metric topology. Denote $B(u, r) = \{v : d(u, v) < r\}$ as the open ball in (\mathcal{M}, d) where u is the center and $r \geq 0$ is the radius. Let $\bar{B}(u, r) = \{v : d(u, v) \leq r\}$ be the corresponding closed ball. For $\forall u, v \in \mathcal{M}$, the metric distribution function of μ on \mathcal{M} is defined as

$$F^M(u, v) = \mu[\bar{B}\{u, d(u, v)\}] = E\{\delta(u, v, X)\},$$

where $\delta(u, v, x) = \mathbb{1}[x \in \bar{B}\{u, d(u, v)\}]$, $\mathbb{1}(\cdot)$ is the indicator function, and the superscript M indicates the metric space. Based on i.i.d. samples $\{X_1, \dots, X_n\}$ from μ on \mathcal{M} , a natural estimate of MDF is the empirical metric distribution function (EMDF)

$$F_n^M(u, v) = \frac{1}{n} \sum_{i=1}^n \delta(u, v, X_i).$$

The following lemma from Wang et al. (2023) establishes the uniform convergence result for EMDF, indicating it enjoys a Glivenko-Cantelli-type property.

Lemma 1 (Theorem 3 in Wang et al. (2023)). Let $\mathcal{F} = \{\delta(u, v, \cdot) : u, v \in \mathcal{M}\}$ be the collection of indicator functions of closed balls on \mathcal{M} . Let $\{X_1, \dots, X_n\}$ be i.i.d. samples from μ . Define $X_1^n = (X_1, \dots, X_n)$ and $\mathcal{F}(X_1^n) = \{(f(X_1), \dots, f(X_n)) \mid f \in \mathcal{F}\}$. If μ satisfies that $\frac{1}{n} E_X[\log(\text{card}(\mathcal{F}(X_1^n)))] \rightarrow 0$, where $\text{card}(\cdot)$ is the cardinality of a set, then

$$\lim_{n \rightarrow \infty} \sup_{u \in \mathcal{M}, v \in \mathcal{M}} |F_{\mu, n}^M(u, v) - F^M(u, v)| = 0, \text{ a.s.}$$

3 The Metric Kolmogorov Filter

3.1 Method

Let $X_j | Y = +1 \sim \mu_j^+$ and $X_j | Y = -1 \sim \mu_j^-$, where μ_j^+ and μ_j^- represent two unknown Borel probability measures on the metric space (\mathcal{M}_j, d_j) . Define $F_{+j}^M(u, v)$ as the metric distribution function of $d_j(u, v)$ for $u, v \sim \mu_j^+$, and similarly, $F_{-j}^M(u, v)$ for $u, v \sim \mu_j^-$. Apparently, a significant distinction between μ_j^+ and μ_j^- implies X_j contributes to predicting label Y . Due to the one-to-one correspondence between a probability measure and its metric distribution function, we are motivated to consider the following statistical divergence

$$\text{MKS}(\mu_j^+ \| \mu_j^-) = \int_{\mathcal{M}_j} \sup_{v \in \mathcal{M}_j} |F_{+j}^M(u, v) - F_{-j}^M(u, v)| d\mu^+(u)$$

to distinguish μ_j^+ from μ_j^- . It works by first measuring the Kolmogorov-Smirnov divergences between $F_{+j}^M(u, v)$ and $F_{-j}^M(u, v)$ for each fixed ball center $u \sim \mu_j^+$, then integrates them by expectation. This statistic is termed the Metric Kolmogorov-Smirnov (MKS) divergence, which has been first visited in a manuscript of Wang et al. (2021) for homogeneity test. Here we symmetrize MKS to measure the importance of X_j to Y by considering the following nonnegative statistic

$$\omega_j = \text{MKS}(\mu_j^+ \| \mu_j^-) + \text{MKS}(\mu_j^- \| \mu_j^+). \quad (1)$$

Intuitively, ω_j quantifies the marginal association of X_j and Y , that is, the larger ω_j is, the more important X_j is. Conversely, when ω_j tends to zero, it indicates an independent relationship between X_j and Y , as shown by Proposition 2.

Proposition 2. *X_j and Y are statistically independent if and only if $\omega_j = 0$.*

At the sample level, we estimate ω_j based on the empirical metric distribution. For ease of presentation, let \mathcal{X}^+ be a dataset containing n_1 i.i.d. samples with positive labels. Thus for $i \in \{1, \dots, n_1\}$ and $j \in \{1, \dots, p\}$, the i th random tuple is denoted as $X_i^+ \in \mathcal{X}^+$, with the j th object $X_{i,j}^+ \sim \mu_j^+$. Similarly, denote \mathcal{X}^- as a dataset containing n_2 samples with negative labels. The complete dataset is then $\mathcal{X} = \mathcal{X}^+ \cup \mathcal{X}^-$, and the total sample size $n = n^+ + n^-$. We utilize

$$\widehat{\text{MKS}}(\mu_j^+ \| \mu_j^-) = \frac{1}{n^+} \sum_{i=1}^{n^+} \max_{v \in \mathcal{X}} |F_{+j, n^+}^M(X_{i,j}^+, v) - F_{-j, n^-}^M(X_{i,j}^+, v)|$$

and

$$\widehat{\text{MKS}}(\mu_j^- \| \mu_j^+) = \frac{1}{n^-} \sum_{i=1}^{n^-} \max_{v \in \mathcal{X}} |F_{-, n^-}^M(X_{i,j}^-, v) - F_{+, n^+}^M(X_{i,j}^-, v)|$$

to estimate ω_j , that is,

$$\widehat{\omega}_j = \widehat{\text{MKS}}(\mu_j^+ \| \mu_j^-) + \widehat{\text{MKS}}(\mu_j^- \| \mu_j^+). \quad (2)$$

Now we define $\mathcal{S} = \{j : \omega_j > 0, j = 1, \dots, p\}$ as the selected set that contains all important features, with cardinality s . In binary classification, we further suppose \mathcal{S} equals to the informative set \mathcal{D} , or more conservatively, $\mathcal{D} \subseteq \mathcal{S}$. This assumption is essential for our theoretical study and aligns with similar assumptions in Euclidean screening literature; see Theorem 1 in Mai and Zou (2013) for reference. To estimate \mathcal{S} , we rank all random objects X_j based on $\widehat{\omega}_j$ and select those among the \hat{s} th largest, where a theoretical choice of \hat{s} is the integer $\lceil n/\log(n) \rceil$. Equivalently, we can also specify a threshold T to filter out uninformative features, resulting

$$\widehat{\mathcal{S}}(T) = \{j : \widehat{\omega}_j \geq T, \text{ for } 1 \leq j \leq p\}. \quad (3)$$

In this case, we slightly abuse notation by using $\hat{s}(T)$ to represent the size of $\widehat{\mathcal{S}}$ when employing a threshold T . We term the above procedure the Metric Kolmogorov filter (MK-Filter), considering $\widehat{\omega}_j$ is constructed based on a symmetrized metric Kolmogorov-Smirnov divergence.

3.2 Sure screening property

The MK-Filter is designed to identify the underlying informative set with high probability. We demonstrate this by showing that the MF-Filter enjoys the sure screening property, a key characteristic commonly shared by various Euclidean screening techniques. To establish the theoretical groundwork for subsequent discussions, we first introduce the following lemma, which provides a uniform concentration inequality for the EMDF.

Lemma 3 (A uniform concentration inequality). *Let μ be a probability measure defined on the metric space (\mathcal{M}, d) and $\{X_1, \dots, X_n\}$ be i.i.d. observations sampled from μ . For each $\epsilon > 0$, there exists a universal constant $N(\epsilon) \in \mathbb{N}$ such that for all $n \geq N(\epsilon)$, we have*

$$\mathbb{P} \left\{ \frac{1}{n} \sum_{i=1}^n \sup_{v \in \mathcal{M}} |F_{\mu, n}^M(X_i, v) - F_{\mu}^M(X_i, v)| > \epsilon \right\} \leq 2 \exp\left(-\frac{n\epsilon^2}{32}\right).$$

Lemma 3 extends the classical Dvoretzky–Kiefer–Wolfowitz inequality (Dvoretzky et al., 1956) to metric spaces, showing that the EMDF exhibits uniform concentration over the sample set at an exponential rate. This finding parallels Corollary 3 in Wang et al. (2023), but instead of taking the supremum, we compute the sample average across various ball centers, thus leading to a slightly improved bound. Using this result, Lemma 4 establishes the consistency of $\widehat{\omega}_j$, followed by demonstrating the sure screening property in Theorem 5.

Lemma 4. *Under the conditions of Lemma 3, for $\widehat{\omega}_j$ defined by (2), we have $\mathbb{P}(|\widehat{\omega}_j - \omega_j| \geq cn^{-\kappa}) \leq O(\exp\{-Cn^{1-2\kappa}\})$ with $0 < \kappa < 1/2$.*

Theorem 5 (Sure screening property). *Define $\xi(\epsilon) = 4 \exp(-\frac{n\pi_y \epsilon^2}{256}) + 2 \exp(-\frac{n\pi_y \epsilon^2}{256}) + \exp(-\frac{c_1 n \pi_y^2}{4}) + \exp(-\frac{c_2 n \pi_y^2}{4})$, where $\pi_y = \mathbb{P}(Y = y)$ for $y = +1, -1$. Assume there exists a selective set S such that the informative set $D \subseteq S$. Let $\delta_S = \min_{j \in S} \omega_j - \max_{j \in S^c} \omega_j > 0$. Then we have $\mathbb{P}\{D \subseteq \widehat{S}(d_n)\} \geq 1 - p\xi(\delta_S/2)$. Thus, if $\delta_S \gg \{\log(p)/n\}^{1/2}$, the sure screening property holds with probability going to 1.*

3.3 A data-adaptive threshold for FDR controlling

The MK-Filter yields a selected set $\widehat{S}(T)$ with a given threshold T , where T controls the set size and, consequently, influences the filtering procedure’s quality. Generally, a conservative strategy tends to choose a small value of T to include all informative features with high probability. While ensuring the sure screening property, this strategy also elevates the risk of retaining more uninformative predictors. As a more reliable approach, we propose controlling the false discovery rate (FDR, Benjamini and Hochberg (1995)) for MK-Filter through a data-adaptive threshold selection procedure. Our approach is inspired by Guo et al. (2023) but is adapted for handling Non-Euclidean features.

Mathematically, $\widehat{S}(T)$ makes a false discovery if there exists a $j \in \widehat{S}(T) \cap S^c$, where S^c denotes the underlying true uninformative set. The false discovery rate is then defined as

$$E[\text{FDP}\{\widehat{S}(T)\}],$$

where

$$\text{FDP}\{\widehat{S}(T)\} = \frac{\#\{j : j \in \widehat{S}(T) \cap S^c\}}{\#\{j : j \in \widehat{S}(T)\}},$$

stands for the false discovery proportion (FDP). With a pre-specified level α , we say using threshold T controls the FDR asymptotically if $\limsup_{n \rightarrow \infty} E[\text{FDP}\{\widehat{S}(T)\}] \leq \alpha$.

We take a data splitting strategy to determine the threshold T for FDR control. Firstly, the whole dataset \mathcal{X} is randomly divided into disjoint parts \mathcal{X}_1 and \mathcal{X}_2 of different sample sizes $n_1 = n(K-1)/K$

and $n_2 = n/K$, where $K \geq 3$ and n/K are assumed to be integers for simplicity. Let $\widehat{\omega}_{j_1}$ and $\widehat{\omega}_{j_2}$ be the symmetrized Metric Kolmogorov-Smirnov statistics calculated on \mathcal{X}_1 and \mathcal{X}_2 respectively. Define

$$W_j = \text{sign}(n_1^\gamma \widehat{\omega}_{1j} - n_2^\gamma \widehat{\omega}_{2j}) \max(n_1^\gamma \widehat{\omega}_{1j}, n_2^\gamma \widehat{\omega}_{2j}), \quad (4)$$

then a data-adaptive threshold is obtained via

$$T = \inf \left\{ t > 0 : \frac{1 + \#\{j : W_j \leq -t\}}{\max(\#\{j : W_j \geq t\}, 1)} \leq \alpha \right\}. \quad (5)$$

Combined with this data-adaptive threshold selection procedure, the MK-Filter works as follows.

Algorithm 1: The MK-Filter with a data-adaptive threshold.

1. Randomly divide the dataset \mathcal{X} into disjoint parts \mathcal{X}_1 and \mathcal{X}_2 ;
 2. Calculate $\widehat{\omega}_{1j}$ and $\widehat{\omega}_{2j}$ on \mathcal{X}_1 and \mathcal{X}_2 separately using (2) for $j = 1, \dots, p$;
 3. Obtain W_j via (4) and choose the threshold T by (5);
 4. Output $\widehat{\mathcal{S}}(T) = \{j : W_j \geq T\}$.
-

Prior to delving into the details of our threshold selection procedure, we present a short discussion on the statistic W_j defined in formula (4), which distinguishes between the behaviors of informative and uninformative predictor X_j . Specifically, for $j \in \mathcal{S}$, by Lemma 4 we have $\widehat{\omega}_j \xrightarrow{P} \omega_j > 0$, thus $W_j > 0$ with probability tending to one, given that $n_1^\gamma \widehat{\omega}_{1j} > n_2^\gamma \widehat{\omega}_{2j} > 0$. Conversely, for $j \in \mathcal{S}^c$, W_j is asymptotically symmetric about zero due to the independence of \mathcal{X}_1 and \mathcal{X}_2 . Since this marginal symmetry property holds for all uninformative predictors, we can use $\#\{j : W_j \leq -t\}$ to approximate both $\#\{j \in \mathcal{S}^c : W_j \leq -t\}$ and $\#\{j \in \mathcal{S}^c : W_j \geq t\}$. Additional theoretical insights into W_j and T are available in Guo et al. (2023).

We demonstrate that Algorithm 1 enables the MF-Filter to control the false discovery rate asymptotically under mild conditions. For clarity, we introduce following notations. Let $\delta_n = cn^{-\kappa}$ and $\xi(\delta_n) = \exp(-Cn\delta_n^2)$, where constants $c > 0$, $C > 0$, and $0 < \kappa < 1/2$. Define $\mathcal{C}_\beta = \{j \in \mathcal{S} : \omega_j > 2\delta_n a/(a-1)\}$, with β representing the cardinality of \mathcal{C} and $a = (K-1)^{1/2}$. Conceptually, the set \mathcal{C}_β collects predictors with identifiable signal strengths. We also define $G_+(t) = (p-s)^{-1} \sum_{j \in \mathcal{S}^c} \mathbb{P}(W_j \geq t)$ and $G_-(t) = (p-s)^{-1} \sum_{j \in \mathcal{S}^c} \mathbb{P}(W_j \leq -t)$. The following technical conditions, introduced in Guo et al. (2023), are required to guarantee the result in proposition 6. Intuitively, the fraction in Condition 1 estimates the false discovery proportion, while the Condition 1 characterizes the convergence of empirical distribution $\{(p-s)G_+(t)\}^{-1} \sum_{j \in \mathcal{S}^c} \mathbb{1}(W_j \geq t)$ and $\{(p-s)G_-(t)\}^{-1} \sum_{j \in \mathcal{S}^c} \mathbb{1}(W_j \leq -t)$.

Condition 1. For $j \in \mathcal{S}^c$, we have $n^{1/2}\widehat{\omega}_j \xrightarrow{d} \mathcal{N}_j$ and $\mathbb{P}(n^{1/2}\widehat{\omega}_j > t)/(1 - F_{\mathcal{N}_j}) \rightarrow 1$ uniformly in $j \in \mathcal{S}^c$ and $t \in (0, n^{1/2})$, as $n \rightarrow \infty$ and $t \rightarrow \infty$, where \mathcal{N}_j is some nondegenerate random variable with distribution function $F_{\mathcal{N}_j}$.

Condition 2. For $\beta \rightarrow \infty$, we have

$$\sup_{0 \leq t \leq G_+^{-1}(\alpha\beta/p)} \left| \{(p-s)G_+(t)\}^{-1} \sum_{j \in \mathcal{S}^c} \mathbb{1}(W_j \geq t) - 1 \right| = o(1)$$

and

$$\sup_{0 \leq t \leq G_-^{-1}(\alpha\beta/p)} \left| \{(p-s)G_-(t)\}^{-1} \sum_{j \in \mathcal{S}^c} \mathbb{1}(W_j \leq -t) - 1 \right| = o(1).$$

Proposition 6. Assume $p = \exp\{o(n^{1-2\kappa})\}$ and Condition 1-2 holds. If $\beta \rightarrow \infty$, $(p-s)\xi(\delta_n) \rightarrow 0$ and $(1-1/K)^{1/2}\delta_n \rightarrow 0$ as $(n, p) \rightarrow \infty$, then Algorithm 1 yields a set $\mathcal{S}(T)$ that ensures $\limsup_{(n,p) \rightarrow \infty} \text{FDR} \leq \alpha$ for any $\alpha \in (0, 1)$.

4 Simulations

4.1 Distributional predictors

It is interesting to compare the MK-Filter with existing Euclidean screening methods. Consider a feature vector $X = (X_1, \dots, X_p)^T \in \mathbb{R}^p$ and a label $Y \in \{-1, +1\}$. In this scenario, classical methods such as Kolmogorov-Filter (Mai and Zou, 2013), MV-SIS (Cui et al., 2015), DC-SIS (Zhu et al., 2011), and Ball-SIS (Pan et al., 2019) can be readily applied. Meanwhile, applying the MK-Filter necessitates specifying a suitable metric space first. A reasonable choice is the Wasserstein space (\mathcal{W}, d_w) of univariate distributions, as described in Section 2.1. Here, for each $i \in \{1, \dots, n\}$ and $j \in \{1, \dots, p\}$, we denote the i th sample of the j th feature with the label $Y_i = y$ as $X_{i,j}^y$. Then, its distribution function $F_{i,j}^y$ can be treated as an object in (\mathcal{W}_j, d_w) .

As discussed earlier, the MK-Filter identifies the informative set by ranking $\widehat{\omega}_j$ for each feature X_j , which relies on estimating the metric distribution functions F_{+j,n^+}^M and F_{-j,n^-}^M . A crucial step in this process involves computing Wasserstein distances $d_w(F_{i,j}^y, F_{i',j}^{y'})$ for pairs of random objects $F_{i,j}^y$ and $F_{i',j}^{y'}$. In practice, however, these $F_{i,j}^y$ and $F_{i',j}^{y'}$ are distribution functions that are often not fully observed, requiring estimation. A straightforward yet effective approach is to use the empirical distribution functions. To be specific, we use m_{yj} observations $\{X_{i,j}^l\}_{l=1}^{m_{yj}}$ with label y to obtain the estimate $\widehat{F}_{i,j}^y$, where $\widehat{F}_{i,j}^y(t) = \sum_{l=1}^{m_{yj}} \mathbb{1}_{(-\infty, t]}(X_{i,j}^l) / m_{yj}$ for all $t \in \mathbb{R}$. We then estimate $d_w(F_{i,j}^y, F_{i',j}^{y'})$ by $d_w(\widehat{F}_{i,j}^y, \widehat{F}_{i',j}^{y'})$, see Fournier and Guillin (2015) and Lei (2020) for the theoretical justification. Without loss of generality, we further set $m_{+j} = m_{-j} = m$, simplifying the computation to $d_w(\widehat{F}_{i,j}^y, \widehat{F}_{i',j}^{y'}) = [\sum_{l=1}^m \{X_{i,j}^{(l)} - X_{i',j}^{(l)}\}^2]^{1/2}$. Here, $X_{i,j}^{(l)}$ and $X_{i',j}^{(l)}$ represent the l th order statistics of the sample sets $\{X_{i,j}^l\}_{l=1}^m$ and $\{X_{i',j}^l\}_{l=1}^m$, respectively.

We consider the following model in our simulation. Suppose Y is generated from the discrete uniform distribution with two categories $\{+1, -1\}$ where $\mathbb{P}(Y = +1) = 1/2$. Given $Y = y$, the p -dimensional feature vector $X = (X_1, \dots, X_p)^T$ is generated as follows.

1. $X_1^+ \sim N(0.3, 1)$ and $X_1^- \sim N(-0.3, 1)$;
2. $X_2^+ \sim \text{Uniform}(-1, 1)$ and $X_2^- \sim \text{Uniform}(-0.8, 1.2)$;
3. $X_3^+ \sim N(0, 1)$ and $X_3^- \sim N(0, 1.5)$;
4. $X_4^+ \sim \text{Uniform}(-1, 1)$ and $X_4^- \sim \text{Uniform}(-1.4, 1.4)$;
5. $X_5^+ \sim N(0, 1)$ and $X_5^- \sim t(3)$;
6. $X_6^+ \sim t(3)$ and $X_6^- \sim t(1)$;
7. $X_7^+ \sim \text{GEV}(\mu, \sigma_1, \xi)$ and $X_7^- \sim \text{GEV}(\mu, \sigma_2, \xi)$, where $\mu = 0$, $\sigma_1 = 0.1$, $\sigma_2 = 0.2$, and $\xi = 0$;
8. $X_8^+ \sim \text{GEV}(\mu, \sigma, \xi_1)$ and $X_8^- \sim \text{GEV}(\mu, \sigma, \xi_2)$, where $\mu = 0$, $\sigma = 0.1$, $\xi_1 = 0.1$, and $\xi_2 = 0.4$;
9. Both X_j^+ and $X_j^- \sim N(0, 1)$ for $j \in \{9, \dots, p\}$.

Clearly, the first 8 features are informative. Setting 1-2, for example, characterize the mean differences between the distribution of X_j^+ and X_j^- . Setting 3-4 represent instances with the identical means but varying degrees of variation. Setting 5-6 stress heavy-tailed cases, comparing Student's t -distributions with different degrees of freedom. Lastly, Setting 7-8 explore generalized extreme value distributions, varying in scales (controlled by σ) or shapes (controlled by ξ).

We compare our MK-Filter with the Kolmogorov-Filter (Mai and Zou, 2013), MV-SIS (Cui et al., 2015), DC-SIS (Zhu et al., 2011), and Ball-SIS (Pan et al., 2019). To handle a feature dimension of $p = 10000$, the MK-Filter employs $m = 20$ samples to compute each $\widehat{F}_{i,j}^y$, resulting in a dataset of $n = 40$ random objects. To ensure fair comparison, all other Euclidean screening methods use $n \times m = 800$ samples for their estimation. To evaluate the effectiveness of each method, we compute the minimum

model size (MMS, FAN and SONG (2010)) to include all informative features. Additionally, we compute the proportion \mathcal{P}_j^s of a single informative feature X_j within a selected set of size s , across 400 repeated experiments. Table 1 summarizes the quantiles of MMS, along with \mathcal{P}_j^s ($j = 1, \dots, 8$) for a given model size $s = \lceil n/\log n \rceil$, where $\lceil x \rceil$ represents the integer part of x .

Table 1: Simulation results for distributional predictors.

	\mathcal{P}_1^s	\mathcal{P}_2^s	\mathcal{P}_3^s	\mathcal{P}_4^s	\mathcal{P}_5^s	\mathcal{P}_6^s	\mathcal{P}_7^s	\mathcal{P}_8^s	Quantile of MMS		
									25%	50%	75%
Kolmogorov-Filter	1	1	0.28	0.98	0	0.02	0.99	0.02	608	1311	2110
MV-SIS	1	1	0.38	0.83	0	0.02	1	0.04	659	1154	1860
DC-SIS	1	1	0.86	0.98	0.04	0.69	1	0.64	47	101	316
Ball-SIS	1	1	1	1	0.24	0.94	1	0.09	77	212	534
MK-Filter	1	1	0.96	0.96	0.93	1	1	0.96	8	8	10

We can see from Table 1 that all methods demonstrate excellent performance in detecting mean differences. However, the Kolmogorov-Filter and MV-SIS show less effectiveness when handling normal distributions with the same mean but slightly different variances, while most methods struggle in heavy-tailed settings. Our method consistently exhibits screening efficiency comparable to or better than others across all scenarios. This positive outcome can be reasonably attributed to the effective characterization of subtle distributional differences by the Wasserstein distance. Our MK-Filter, designed for use in metric spaces, seamlessly integrates with Wasserstein distance, resulting in satisfactory performance across various distributional differences.

4.2 Symmetric positive definite matrices

We consider a scenario where features consist of symmetric positive definite matrices. Given the label $Y = y$, assume each random object X_j of the p -tuple features $X = (X_1, \dots, X_p)$ follows a Wishart distribution, denoted as $X_j^y \sim \mathcal{W}_m(v_m, \Sigma_y) \in \mathbb{R}^{m \times m}$, where $v_m > m - 1$ represents the degree of freedom, and $\Sigma_y > 0$ is the scale matrix. We generate Y from the discrete uniform distribution with $\mathbb{P}(Y = +1) = \mathbb{P}(Y = -1) = 1/2$, then draw X_j from the following models.

1. For $j \in \{1, 2\}$, $X_j^+ \sim \mathcal{W}_m(v_m, I_m)$ and $X_j^- \sim \mathcal{W}_m(v_m, 0.6 * I_m)$;
2. For $j \in \{3, 4\}$, $X_j^+ \sim \mathcal{W}_m(v_m, I_m)$ and $X_j^- \sim \mathcal{W}_m(v_m, \text{AR}_m(0.4))$;
3. For $j \in \{5, 6\}$, $X_j^+ \sim \mathcal{W}_m(v_m, I_m)$ and $X_j^- \sim \mathcal{W}_m(v_m, \text{HC}_m(0.5, \Lambda_m))$;
4. For $j \in \{7, 8\}$, $X_j^+ \sim \mathcal{W}_m(v_m, \text{AR}_m(-0.25))$ and $X_j^- \sim \mathcal{W}_m(v_m, \text{AR}_m(0.25))$;
5. For $j \in \{9, 10\}$, $X_j^+ \sim \mathcal{W}_m(v_m, \text{HC}_m(0.2, \Lambda_m))$ and $X_j^- \sim \mathcal{W}_m(v_m, \text{HC}_m(0.5, \Lambda_m))$;
6. For $j \in \{11, \dots, p\}$, both X_j^+ and $X_j^- \sim \mathcal{W}_m(v_m, \Sigma_m)$, where Σ_m is randomly chosen from I_m , $\text{AR}_m(-0.2)$, $\text{AR}_m(0.5)$, or $\text{HC}_m(0.5, \Lambda_m)$.

In the above settings, I_m denotes a $m \times m$ identity covariance matrix, and $\text{AR}_m(\rho)$ denotes a $m \times m$ autoregressive covariance matrix, with the (k, l) th element $\Sigma_{k,l} = \rho^{|k-l|}$. Similarly, $\text{HC}_m(\rho, \Lambda_m)$ represents a $m \times m$ heterogeneous compound covariance matrix with (k, l) th element $\Sigma_{k,l} = \rho \lambda_k \lambda_l$ for $k \neq l$ and $\Sigma_{k,l} = \lambda_k^2$ for $k = l$, where $k, l = 1, \dots, m$ and λ_k is the k th element of the diagonal matrix Λ_m .

We use three different metrics to measure the distance between X_j^+ and X_j^- , namely, the Euclidean metric

$$d_E(X_j^+, X_j^-) = \|X_j^+ - X_j^-\|_F,$$

the Cholesky metric

$$d_C(X_j^+, X_j^-) = \|\text{chol}(X_j^+) - \text{chol}(X_j^-)\|_F,$$

and the Log-Cholesky metric proposed by Lin (2019),

$$d_{LC}(X_j^+, X_j^-) = \left[\|\llbracket \text{chol}(X_j^+) \rrbracket - \llbracket \text{chol}(X_j^-) \rrbracket\|_F^2 + \|\log \mathbb{D}\{\text{chol}(X_j^+)\} - \log \mathbb{D}\{\text{chol}(X_j^-)\}\|_F^2 \right]^{1/2}.$$

Here, $\|A\|_F = \{\text{tr}(A^T A)\}^{1/2}$ denotes the Frobenius norm of matrix A , $\text{chol}(A)$ represents the lower triangular matrix L in the Cholesky decomposition $A = LL^T$, $\llbracket A \rrbracket$ denotes the strictly lower triangular part of A , and $\mathbb{D}(A)$ is the diagonal part of A .

In our experiments, we consider $m = 3$ and $m = 5$ separately, with $v_3 = v_5 = 10$, $\Lambda_3 = \text{diag}(1, 1.1, 1.2)$, and $\Lambda_5 = \text{diag}(1, 1.05, 1.1, 1.15, 1.2)$. For each setting, we fix $p = 2000$ and generate $n = 100$ observations. We control the FDR using the threshold given by Algorithm 1, with significant level $\alpha = 0.1$ and 0.2 , respectively. We evaluate the performance of MK-Filter by computing the quantiles of MMS and the proportions \mathcal{P}_j^s for $j = 1, 3, 5, 7, 9$ based on 400 replicates. The size of informative set is controlled by the threshold computed using Algorithm 1. Additionally, we calculate the false discovery rate for each setting. Results are presented in Table 2 and 3.

Table 2: Simulation results of the MF-Filter with different metrics for \mathcal{S}_3^+ features.

		FDR	\mathcal{P}_1^s	\mathcal{P}_3^s	\mathcal{P}_5^s	\mathcal{P}_7^s	\mathcal{P}_9^s	Quantile of MMS		
								25%	50%	75%
$\alpha = 0.1$	Euclidean	0.053	0.871	0.7	0.279	0.686	0.307	11	14	23
	Cholesky	0.03	0.493	0.8	0.3	0.714	0.457	10	10	11
	Log-Cholesky	0.027	0.414	0.743	0.293	0.693	0.457	10	10	11
$\alpha = 0.2$	Euclidean	0.099	0.929	0.764	0.364	0.714	0.379	12	16	25
	Cholesky	0.092	0.671	0.9	0.507	0.893	0.657	10	10	12
	Log-Cholesky	0.088	0.643	0.893	0.507	0.914	0.629	10	10	12

Table 3: Simulation results of the MF-Filter with different metrics for \mathcal{S}_5^+ features.

		FDR	\mathcal{P}_1^s	\mathcal{P}_3^s	\mathcal{P}_5^s	\mathcal{P}_7^s	\mathcal{P}_9^s	Quantile of MMS		
								25%	50%	75%
$\alpha = 0.1$	Euclidean	0.072	0.929	0.857	0.557	0.786	0.557	10	10	10
	Cholesky	0.038	0.7	0.857	0.4	0.821	0.614	10	10	10
	Log-Cholesky	0.037	0.75	0.936	0.436	0.85	0.636	10	10	10
$\alpha = 0.2$	Euclidean	0.166	1	0.957	0.714	0.936	0.771	10	10	11
	Cholesky	0.186	0.879	0.964	0.636	0.936	0.843	10	10	10
	Log-Cholesky	0.169	0.9	0.986	0.764	0.95	0.864	10	10	10

In both tables, we observe that the actual false discovery rates are below the corresponding nominal levels, indicating the effectiveness of Algorithm 1. The MMS of MK-Filter also closely approximate the true informative set size for all three metrics. Additionally, the proportions of informative features are selected significantly increase when using the Cholesky metric or Log-Cholesky metric, except for \mathcal{P}_1^s . This can be understood by noticing that in Setting 1, we are comparing two $m \times m$ identity covariance matrices of different scales, which can also be seen as degenerate m -dimensional vectors. The Euclidean metric is more suitable in this case because it does not involve misleading correlations among different elements. For all other settings, both Cholesky and Log-Cholesky metrics are preferable due to their attractive geometric properties.

5 Application: abnormal connectivity detection in autism brains

5.1 Study background

Autism is a neurodevelopmental disorder characterized by deficits in social interaction and repetitive behaviors (Muhle et al., 2004). While its neurobiology largely remains unknown, subtle alterations in brain regions, along with resulting abnormal functional connectivity patterns, are believed to play a crucial role in understanding autism (Ha et al., 2015; Postema et al., 2019; Dekhil et al., 2021). Researchers often explore these patterns by constructing covariance matrices of blood-oxygen-level dependent signals derived from brain activities in specific regions, using resting-state functional magnetic resonance imaging (fMRI) observations (Friston, 2011). Such covariance matrices naturally form features in \mathcal{S}^+ when equipped with a suitable metric.

Traditional autism studies typically begin by selecting a set of m regions of interest and then analyze their functional connectivities. However, our study suggests to take a different angle. We directly examine all possible $m \times m$ covariance matrices, representing interactions among arbitrary m regions. This comprehensive exploration results in a large pool of potential features in metric spaces. We then apply the MK-Filter to identify informative features, specifically covariance matrices representing abnormal connectivities in autistic brains. The altered regions are identified by locating elements in these informative matrices. This inverse study procedure thoroughly investigates $m \times m$ functional connectivities without any omissions, aligning with the whole-brain analysis advocated by Müller et al. (2011) and others. We ensure the significance of our findings by controlling the false discovery rate. This meticulous filtering process aims to uncover previously unknown abnormal brain connectivities, offering valuable insights for further investigation.

We analyze resting-state fMRI data from the Autism Brain Imaging Data Exchange (ABIDE, Di Martino et al. (2014)). Our main goal is to use the proposed MK-Filter to identify distinct brain functional connectivities between individuals with autism and controls. These detected abnormal connectivities can further serve as informative features for detecting autism. Below, we describe our procedure in detail.

5.2 Data processing

In this study, we utilize 149 fMRI samples from the ABIDE data collected at the NYU station, comprising 51 samples from subjects with autism and 98 from controls. All samples have been preprocessed using the Python package nilearn (Abraham et al., 2014), employing the Configurable Pipeline for the Analysis of Connectomes (C-PAC, Craddock et al. (2013)). Each preprocessed sample is a tensor of dimension $61 \times 73 \times 61 \times 176$, representing a time series of length 176, with each time index corresponding to an fMRI measurement voxel of size $61 \times 73 \times 61$.

Based on the Harvard-Oxford cortical and subcortical structural atlases (Desikan et al., 2006), the entire brain is segmented into 48 cortical regions, denoted by $\mathcal{R} = \{R_1, \dots, R_{48}\}$. Notice here we chose the Harvard-Oxford atlases for ease of illustration; however, other brain parcellation methods can also be utilized. Given this parcellation, the preprocessed voxel-specific time series are divided into 48 groups according to related regions and averaged, resulting in a 48×176 array of fMRI measurements.

5.3 Construct a feature pool of SPD matrices

For each subject $i \in \{1, \dots, 149\}$, we compute a 48×48 covariance matrix Σ_i using the corresponding 48×176 fMRI data. Such a matrix characterizes the functional connectivity of the entire brain and potentially contains information about abnormal brain connectivity related to autism, although might be obscured. To detect subtle differences in local connectivities, we explore pairwise and triplewise connectivities between different brain regions, represented by covariance matrices of size 2×2 and 3×3 , respectively. These matrices are easily obtained by selecting corresponding elements in Σ_i . For instance, utilizing the interactions of the j th and k th rows and columns of Σ_i , we derive a 2×2 sub-matrix denoted as $\Sigma_i(R_j, R_k)$, characterizing the functional connectivity between regions R_j and R_k , where $R_j, R_k \in \mathcal{R}$.

Treating $\Sigma_i(R_j, R_k)$ and $\Sigma_{i'}(R_j, R_k)$, calculated from the subject i with autism and i' the control, as random objects in \mathcal{S}_2^+ , various distances can be employed to compare their similarities. Here, we employ the log-Cholesky metric $d_{LC}(\cdot, \cdot)$ for its nice properties (Lin, 2019). Roughly speaking, when $d_{LC}\{\Sigma_i(R_j, R_k), \Sigma_{i'}(R_j, R_k)\}$ is notably large, it suggests significant differences between $\Sigma_i(R_j, R_k)$ and $\Sigma_{i'}(R_j, R_k)$, implying that $\Sigma(R_j, R_k)$ might be an informative feature for detecting autism. This inspires us to examine all such 2×2 matrices. Considering combinations of selecting 2 regions from the set \mathcal{R} of 48 elements, we obtain $C_{48}^2 = 1128$ covariance matrices, resulting in a collection of features $\mathcal{X}_2 = \{\Sigma(R_j, R_k) \in \mathcal{S}_2^+ : R_j, R_k \in \mathcal{R}, \text{ and } j \neq k\}$. Similarly, we take $\Sigma(R_j, R_k, R_l)$ to describe the triplewise connectivities among regions R_j, R_k , and R_l . Combining all such 3×3 sub-matrices also constructs a feature pool $\mathcal{X}_3 = \{\Sigma(R_j, R_k, R_l) \in \mathcal{S}_3^+ : R_j, R_k, R_l \in \mathcal{R}, \text{ and } j \neq k \neq l\}$ of size $C_{48}^3 = 17296$. The whole procedure is illustrated in Figure 1. Detecting autism based on these large-scale features is challenging, given the limited sample size of $n = 149$. This motivates us to first obtain an informative feature set.

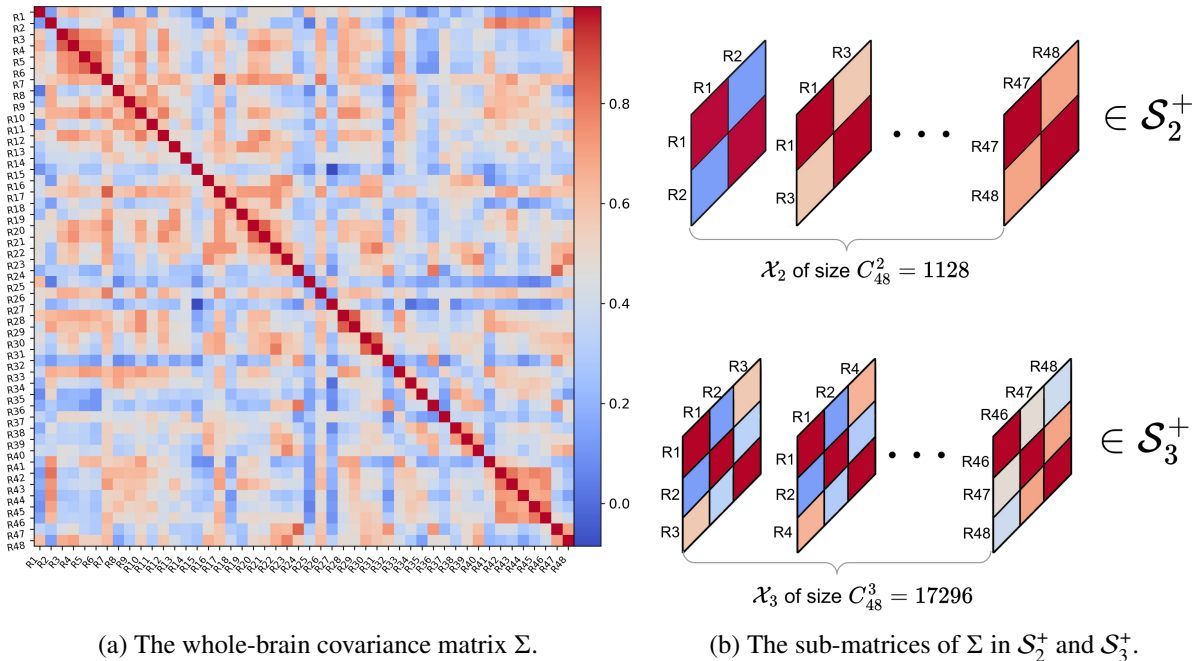


Figure 1: A feature pool derived from the whole-brain covariance for autism detection. Panel (a) displays the covariance matrix of 48 brain regions of interest, utilizing fMRI data from a chosen subject. Panel (b) illustrates C_{48}^2 random objects in \mathcal{S}_2^+ and C_{48}^3 objects \mathcal{S}_3^+ as potential features, which represent combinations of sub-matrices derived from Σ , with size 2×2 and 3×3 , respectively.

5.4 Abnormal connectivities detection

We apply the MK-Filter to (\mathcal{X}_2, d_{LC}) and (\mathcal{X}_3, d_{LC}) , respectively. With significant level $\alpha = 0.1$, a few covariance matrices are identified as informative features that effectively differentiate functional connectivities between individuals with and without autism, as shown in Table 4.

The last column of Table 4 lists significantly altered brain regions in autism compared with controls. Some, such as frontal pole, middle temporal gyrus, and parahippocampal gyrus, have been widely reported in MRI-based autism studies to show reduced connectivity to other regions (see Rane et al. (2015) for a detailed review). Others, like temporal pole and cuneal cortex, have been less frequently reported and may warrant future investigation. Importantly, our findings extend beyond individual brain region analyses, directly identifying abnormal interactions among brain regions in autism. In this case study, the abnormal connectivities are filtered from an exhaustive analysis of 1128 pairwise and 17296 triplewise interactions, covering all conceivable combinations. Consequently, the reported set of informative fea-

Table 4: Informative features obtained by MK-Filter.

Informative features		Related regions
\mathcal{S}_2^+	$\Sigma(R_1, R_{11})$	R_1 : Frontal Pole; R_8 : Temporal Pole;
	$\Sigma(R_8, R_{32})$	R_{11} : Middle Temporal Gyrus (anterior division); R_{12} : Middle Temporal Gyrus (posterior division);
\mathcal{S}_3^+	$\Sigma(R_1, R_{11}, R_{12})$	R_{13} : Middle Temporal Gyrus (temporooccipital part);
	$\Sigma(R_1, R_{12}, R_{35})$	R_{32} : Cuneal Cortex;
	$\Sigma(R_1, R_{11}, R_{34})$	R_{34} : Parahippocampal Gyrus (anterior division);
	$\Sigma(R_1, R_{11}, R_{13})$	R_{35} : Parahippocampal Gyrus (posterior division).

tures is expected to capture all potentially significant pairwise and triplewise connectivities for detecting autism with a high probability, while controlling the false discovery rate at $\alpha = 0.1$. By precisely identifying the involved brain regions and their related connectivities, our results provide a helpful understanding of the disorder’s neural mechanisms.

The findings presented in Table 4 can also be explained geometrically. Notice the matrix $\Sigma(R_j, R_k)$ takes the form:

$$\Sigma(R_j, R_k) = \begin{pmatrix} a & b \\ b & c \end{pmatrix}, \quad ac - b^2 > 0, \quad a > 0, \quad (6)$$

representing a point $(a, b, c)^T \in \mathbb{R}^3$. All such matrices form a cone \mathcal{S}_2^+ in \mathbb{R}^3 , and \mathcal{X}_2 is a set of points situated in this cone. For each feature $\Sigma(R_j, R_k) \in \mathcal{X}_2$, we compute its sample averages based on different sample classes (i.e., autism or control), resulting in a pair of points within this cone. In Figure 2, red and blue points represent informative features $\Sigma(R_1, R_{11})$ and $\Sigma(R_8, R_{32})$, respectively, while the black points correspond to uninformative features randomly chosen from \mathcal{X}_2 . Here, the symbol “+” denotes the autism class, and the dot represents the control. By comparing the pairs of black points to the red (or blue) points, we observe a larger distance within the latter, indicating more distinct characteristics between autism and control. The use of \mathcal{S}_2^+ serves as an intuitive visual example, but similar conclusions apply to features in \mathcal{S}_3^+ .

5.5 Classification

In the final step, we evaluate the prediction performance using the informative features identified by MK-Filter. The k -Nearest Neighbors (k -NN) classifier is a natural choice for binary classification within a metric space. It predicts the label of a new sample x_0 based on the majority vote of its k closest neighbors, determined by measuring distances or metrics between x_0 and existing samples. In our experiments, we employ the k -NN classifier on two different feature sets: the whole-brain covariance matrix of size 48×48 , or the informative features identified by the MK-Filter in Step 5.4, utilizing the Log-Cholesky metric.

In the second scenario, determining the nearest points of x_0 requires considering multiple features, posing a multivariate ranking challenge. We propose two strategies to address this: the first one is “voting”, which applies the k -NN classifier on each feature separately and then combines the results via voting to obtain the prediction; the second approach, termed “merging”, works by assigning a new metric on the product space of the informative features, thus allowing for a univariate ranking. Specifically, for the tuple $X = (X_1, \dots, X_s)$ comprising informative features $X_j \in (\mathcal{M}_j, d_j)$, $j = 1, \dots, s$, we define a new metric space (\mathcal{M}, d) . Here, $\mathcal{M} = \prod_{j=1}^s \mathcal{M}_j$ represents the Cartesian product of \mathcal{M}_j , and $d(u, v) = \{\sum_{j=1}^s d_1^2(u_j, v_s)\}^{1/2}$ for $u, v \in \mathcal{M}$ is the corresponding metric. The k -NN classifier can then be applied using this metric $d(\cdot, \cdot)$.

We conduct experiments for each setting with k values 3, 6, and 9. In each experiment, the samples are randomly split into training and testing sets in a ratio of 7 : 3, and the classification performance on the testing set is recorded. Table 5 summarizes the averaged results from 400 replicates, with standard

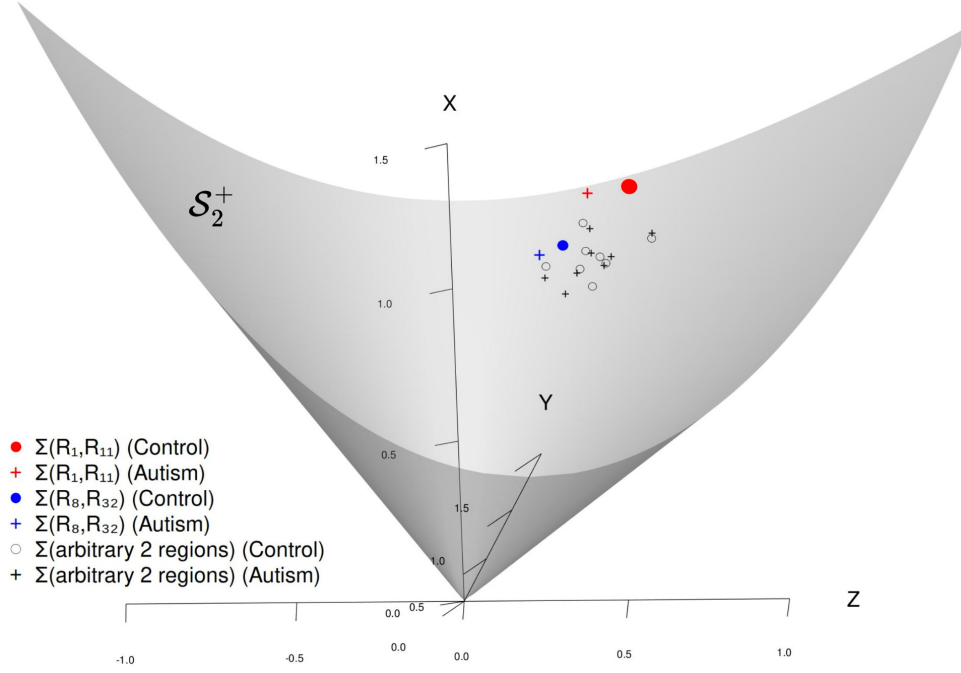


Figure 2: Informative features (marked with red or blue colors) within S_2^+ exhibit more distinct values between individuals with autism (denoted by “+”) and controls (denoted by circles), compared to uninformative counterparts.

errors shown in parentheses. It’s evident that the k -NN classifier using identified informative features exhibits significant improvements for both strategies.

Table 5: The performance of k -NN classifier using different features.

k	Feature	Accuracy	Recall rate	F1-Score
3	Whole-brain	0.652 (0.06)	0.172 (0.09)	0.241 (0.10)
	MK-Filter + merging	0.729 (0.06)	0.523 (0.11)	0.559 (0.09)
	+ voting	0.720 (0.05)	0.559 (0.11)	0.567 (0.08)
6	Whole-brain	0.666 (0.06)	0.270 (0.12)	0.343 (0.12)
	MK-Filter + merging	0.730 (0.05)	0.515 (0.11)	0.559 (0.09)
	+ voting	0.708 (0.06)	0.636 (0.10)	0.594 (0.08)
9	Whole-brain	0.680 (0.06)	0.156 (0.09)	0.239 (0.11)
	MK-Filter + merging	0.723 (0.06)	0.497 (0.11)	0.546 (0.10)
	+ voting	0.723 (0.06)	0.505 (0.13)	0.549 (0.09)

6 Discussion

In this paper, we proposed a filtering method designed to identify informative features for binary classification from a large set of non-Euclidean objects in metric spaces. We conduct a comprehensive analysis, exploring both its theoretical properties and application performance. While our discussion primarily focuses on its effectiveness with SPD matrices, our method’s applicability can be extended to handle a broader range of metric features.

It is worth noting that the effectiveness of our approach hinges on the choice of the metric used to differentiate between various random objects. Selecting an appropriate metric is an essential problem of

independent interest, closely related to the application background, and should be justified case by case.

References

- Alexandre Abraham, Fabian Pedregosa, Michael Eickenberg, Philippe Gervais, Andreas Mueller, Jean Kossaifi, Alexandre Gramfort, Bertrand Thirion, and Gaël Varoquaux. Machine learning for neuroimaging with scikit-learn. *Frontiers in neuroinformatics*, 8:14, 2014.
- Vincent Arsigny, Pierre Fillard, Xavier Pennec, and Nicholas Ayache. Geometric means in a novel vector space structure on symmetric positive-definite matrices. *SIAM journal on matrix analysis and applications*, 29(1):328–347, 2007.
- Yoav Benjamini and Yosef Hochberg. Controlling the false discovery rate: a practical and powerful approach to multiple testing. *Journal of the Royal statistical society: series B (Methodological)*, 57(1):289–300, 1995.
- Satarupa Bhattacharjee and Hans-Georg Müller. Single index fréchet regression. *The Annals of Statistics*, 51(4):1770–1798, 2023.
- Louis J Billera, Susan P Holmes, and Karen Vogtmann. Geometry of the space of phylogenetic trees. *Advances in Applied Mathematics*, 27(4):733–767, 2001.
- Kamalika Chaudhuri and Sanjoy Dasgupta. Rates of convergence for nearest neighbor classification. *Advances in Neural Information Processing Systems*, 27, 2014.
- Yaqing Chen, Zhenhua Lin, and Hans-Georg Müller. Wasserstein regression. *Journal of the American Statistical Association*, 118(542):869–882, 2023.
- Thomas Cover and Peter Hart. Nearest neighbor pattern classification. *IEEE transactions on information theory*, 13(1):21–27, 1967.
- Cameron Craddock, Sharad Sikka, Brian Cheung, Ranjeet Khanuja, Satrajit S Ghosh, Chaogan Yan, Qingyang Li, Daniel Lurie, Joshua Vogelstein, Randal Burns, Stanley Colcombe, Maarten Mennes, Clare Kelly, Adriana Di Martino, Francisco Xavier Castellanos, and Michael Milham. Towards automated analysis of connectomes: The Configurable Pipeline for the Analysis of Connectomes (C-PAC). *Frontiers in Neuroinformatics*, (42), 2013. ISSN 1662-5196.
- Hengjian Cui, Runze Li, and Wei Zhong. Model-free feature screening for ultrahigh dimensional discriminant analysis. *Journal of the American Statistical Association*, 110(510):630–641, 2015.
- Omar Dekhil, Ahmed Shalaby, Ahmed Soliman, Ali Mahmoud, Maiying Kong, Gregory Barnes, Adel Elmaghraby, and Ayman El-Baz. Identifying brain areas correlated with ados raw scores by studying altered dynamic functional connectivity patterns. *Medical Image Analysis*, 68:101899, 2021.
- Rahul S Desikan, Florent Ségonne, Bruce Fischl, Brian T Quinn, Bradford C Dickerson, Deborah Blacker, Randy L Buckner, Anders M Dale, R Paul Maguire, Bradley T Hyman, et al. An automated labeling system for subdividing the human cerebral cortex on mri scans into gyral based regions of interest. *Neuroimage*, 31(3):968–980, 2006.
- Adriana Di Martino, Chao-Gan Yan, Qingyang Li, Erin Denio, Francisco X Castellanos, Kaat Alaerts, Jeffrey S Anderson, Michal Assaf, Susan Y Bookheimer, Mirella Dapretto, et al. The autism brain imaging data exchange: towards a large-scale evaluation of the intrinsic brain architecture in autism. *Molecular psychiatry*, 19(6):659–667, 2014.
- Ian L. Dryden, Alexey Koloydenko, and Diwei Zhou. Non-Euclidean statistics for covariance matrices, with applications to diffusion tensor imaging. *The Annals of Applied Statistics*, 3(3):1102 – 1123, 2009. doi: 10.1214/09-AOAS249. URL <https://doi.org/10.1214/09-AOAS249>.

- Paromita Dubey and Hans-Georg Müller. Functional models for time-varying random objects. *Journal of the Royal Statistical Society Series B: Statistical Methodology*, 82(2):275–327, 2020.
- Aryeh Dvoretzky, Jack Kiefer, and Jacob Wolfowitz. Asymptotic minimax character of the sample distribution function and of the classical multinomial estimator. *The Annals of Mathematical Statistics*, pages 642–669, 1956.
- Jianqing Fan and Jinchi Lv. Sure independence screening for ultrahigh dimensional feature space. *Journal of the Royal Statistical Society Series B: Statistical Methodology*, 70(5):849–911, 2008.
- Jianqing Fan and Jinchi Lv. Sure independence screening. *Wiley StatsRef: Statistics Reference Online*, 2018.
- JIANQING FAN and RUI SONG. Sure independence screening in generalized linear models with np-dimensionality. *The Annals of Statistics*, 38(6):3567–3604, 2010.
- Nicolas Fournier and Arnaud Guillin. On the rate of convergence in wasserstein distance of the empirical measure. *Probability Theory and Related Fields*, 162(3):707–738, 2015.
- Karl J Friston. Functional and effective connectivity: a review. *Brain connectivity*, 1(1):13–36, 2011.
- Lee-Ad Gottlieb, Aryeh Kontorovich, and Robert Krauthgamer. Efficient classification for metric data. *IEEE Transactions on Information Theory*, 60(9):5750–5759, 2014.
- Xu Guo, Haojie Ren, Changliang Zou, and Runze Li. Threshold selection in feature screening for error rate control. *Journal of the American Statistical Association*, 118(543):1773–1785, 2023.
- Sungji Ha, In-Jung Sohn, Namwook Kim, Hyeon Jeong Sim, and Keun-Ah Cheon. Characteristics of brains in autism spectrum disorder: structure, function and connectivity across the lifespan. *Experimental neurobiology*, 24(4):273, 2015.
- Martin Kleiber and William J Pervin. A generalized banach-mazur theorem. *Bulletin of The Australian Mathematical Society*, 1(2):169–173, 1969.
- Aryeh Kontorovich, Sivan Sabato, and Ruth Urner. Active nearest-neighbor learning in metric spaces. *Journal of Machine Learning Research*, 18(195):1–38, 2018.
- Jing Lei. Convergence and concentration of empirical measures under wasserstein distance in unbounded functional spaces. *Bernoulli*, 26(1):767–798, 2020.
- Lek-Heng Lim, Ken Sze-Wai Wong, and Ke Ye. The grassmannian of affine subspaces. *Foundations of Computational Mathematics*, 21:537–574, 2021.
- Yinan Lin and Zhenhua Lin. Logistic regression and classification with non-euclidean covariates. *arXiv preprint arXiv:2302.11746*, 2023.
- Zhenhua Lin. Riemannian geometry of symmetric positive definite matrices via cholesky decomposition. *SIAM Journal on Matrix Analysis and Applications*, 40(4):1353–1370, 2019.
- Qing Mai and Hui Zou. The kolmogorov filter for variable screening in high-dimensional binary classification. *Biometrika*, 100(1):229–234, 2013.
- Kanti V Mardia, Peter E Jupp, and KV Mardia. *Directional statistics*, volume 2. Wiley Online Library, 2000.
- Andrew McCormack and Peter Hoff. Equivariant estimation of fr\'echet means. *arXiv preprint arXiv:2104.03397*, 2021.

- Rebecca Muhle, Stephanie V Trentacoste, and Isabelle Rapin. The genetics of autism. *Pediatrics*, 113(5):e472–e486, 2004.
- Ralph-Axel Müller, Patricia Shih, Brandon Keehn, Janae R Deyoe, Kelly M Leyden, and Dinesh K Shukla. Underconnected, but how? a survey of functional connectivity mri studies in autism spectrum disorders. *Cerebral cortex*, 21(10):2233–2243, 2011.
- Wenliang Pan, Xueqin Wang, Weinan Xiao, and Hongtu Zhu. A generic sure independence screening procedure. *Journal of the American Statistical Association*, 2019.
- Alexander Petersen and Hans-Georg Müller. Fréchet regression for random objects with euclidean predictors. 2019.
- Merel C Postema, Daan Van Rooij, Evdokia Anagnostou, Celso Arango, Guillaume Auzias, Marlene Behrmann, Geraldo Busatto Filho, Sara Calderoni, Rosa Calvo, Eileen Daly, et al. Altered structural brain asymmetry in autism spectrum disorder in a study of 54 datasets. *Nature communications*, 10(1):4958, 2019.
- Pallavi Rane, David Cochran, Steven M Hodge, Christian Haselgrove, David N Kennedy, and Jean A Frazier. Connectivity in autism: a review of mri connectivity studies. *Harvard review of psychiatry*, 23(4):223–244, 2015.
- Ulrike von Luxburg and Olivier Bousquet. Distance-based classification with lipschitz functions. *J. Mach. Learn. Res.*, 5(Jun):669–695, 2004.
- Xueqin Wang, Jin Zhu, Wenliang Pan, Junhao Zhu, and Heping Zhang. Nonparametric statistical inference via metric distribution function in metric spaces. *arXiv e-prints*, pages arXiv–2107, 2021.
- Xueqin Wang, Jin Zhu, Wenliang Pan, Junhao Zhu, and Heping Zhang. Nonparametric statistical inference via metric distribution function in metric spaces. *Journal of the American Statistical Association*, pages 1–13, 2023.
- Chao Ying and Zhou Yu. Fréchet sufficient dimension reduction for random objects. *Biometrika*, 109(4):975–992, 2022.
- Qi Zhang, Lingzhou Xue, and Bing Li. Dimension reduction for fréchet regression. *Journal of the American Statistical Association*, (just-accepted):1–27, 2023.
- Li-Ping Zhu, Lexin Li, Runze Li, and Li-Xing Zhu. Model-free feature screening for ultrahigh-dimensional data. *Journal of the American Statistical Association*, 106(496):1464–1475, 2011.